

# Transitions and time scales to equipartition in oscillator chains: Low-frequency initial conditions

Jayme De Luca<sup>1</sup> and Allan Lichtenberg<sup>2</sup>

<sup>1</sup>*Departamento de Física, Universidade Federal de São Carlos, Rodovia Washington Luiz km 235, 13565-905, Caixa Postal 676, São Carlos-São Paulo, Brazil*

<sup>2</sup>*Department of Electrical Engineering and Computer Sciences, University of California at Berkeley, Berkeley, California 94720*

(Received 11 April 2002; published 19 August 2002)

We study the times to equipartition  $T_{eq}$  in an oscillator chain, which is the discretized Klein-Gordon equation with a quartic nonlinearity ( $\varphi^4$  system). The numerical results are compared to the Fermi-Pasta-Ulam (FPU) oscillator chain with quartic nonlinearity (FPU- $\beta$  system). For both chains we consider initial energies in low-frequency modes, of the linear systems. The methods previously developed to estimate the equipartition times for the FPU- $\beta$  chain are applied to the more complicated  $\varphi^4$  chain. The results indicate that the methods are still applicable, but do not give as accurate predictions of the equipartition time or the transitions between power-law and exponential behavior.

DOI: 10.1103/PhysRevE.66.026206

PACS number(s): 05.45.-a, 63.20.Ry, 63.10.+a

## I. INTRODUCTION

Nonlinear oscillator chains are useful systems to study the foundations of statistical mechanics; in particular to determine the transitions and time scales for relaxation from one or a few modes to equipartition among modes. Beginning with the famous Fermi-Pasta-Ulam (FPU) study [1,2] there have been many numerical and theoretical studies of these phenomena.

The FPU- $\beta$  system is a linear chain of equal masses coupled by nonlinear springs with Hamiltonian (for quartic nonlinearity)

$$H = \sum_{i=1}^N \frac{1}{2} p_i^2 + \frac{1}{2} (q_{i+1} - q_i)^2 + \frac{\beta}{4} (q_{i+1} - q_i)^4. \quad (1)$$

Typically, the energy interchange among the “linearized” system modes for the case of strong springs ( $\beta > 0$ ) and either fixed boundaries  $q_0 = q_{N+1} = 0$  or periodic  $q_0 = q_{N+1}$  has been studied [3–16]. To numerically study the FPU system, initial conditions have been used for which all the energy is concentrated in a few modes usually around a low-frequency mode  $\gamma \ll N$  or around a high-frequency mode  $N - \gamma$  ( $\gamma \ll N$ ).

Numerical measures of the degree of energy sharing among modes have been developed and we present these measures, together with numerical results, in Sec. III. For energy either in a few low-frequency modes or in a few high-frequency modes, we have developed theoretical descriptions for energy spreading among modes, valid in various energy ranges, which were compared to numerical results [8–10]. In earlier works [5,6], the transition studied was between weak and strong stochasticity, with different power-law behavior in the two regimes. The numerically determined transition was related to a theory of overlap of neighboring modes in phase space [4]. Subsequent work [7–10] focused on the region of weak stochasticity with the transition between power law and exponentially long time scales as the energy density  $\varepsilon = E/N$  of the system is decreased. This latter transition is of more importance for the observation of equipartition, as it essentially separates ob-

servable times from those that are not observable. For the FPU chain, the main mechanisms leading to equipartition in this lower-energy regime are that resonant interaction of four low-frequency modes, in which a significant portion of the energy resides, can lead to local superperiod (very low-frequency) beat oscillations that are stochastic. If beat oscillations, which increase with energy, are sufficiently fast they become comparable to frequency differences between high-frequency modes. This results in the Arnold diffusion mechanism transferring energy to high-frequency modes.

For the FPU- $\beta$  chain the transition to stochastic local interaction, using the four-mode approximation for low-frequency modes, occurs at [8]

$$R \equiv (N+1) \frac{6\beta}{\pi^2} E \approx 1,$$

where  $R$  is the ratio of nonlinear to linear energy in a perturbation Hamiltonian. Since  $R \propto N+1$ , the energy at which this transition occurs becomes vanishingly small as  $N \rightarrow \infty$ . The stochasticity at  $R \approx 1$  corresponds to the appearance of an elliptic-hyperbolic pair of fixed points in a low-frequency resonance among the modes. Since the driving frequency for diffusion is associated with the libration frequency of the resonance  $\Omega_B$ , a fundamental time scale for numerical observation is [8]

$$\frac{2\pi}{\Omega_B} \sim \frac{1}{w_\gamma} \frac{N}{\beta E} \approx N^2 / \gamma \beta E_\gamma,$$

where  $E_\gamma \approx E$  if most of the energy is initially in the few modes taking part of the beat oscillation, and we have approximated the linear mode frequency for FPU as  $w_\gamma = \pi \gamma / N$ . Using resonant normal form perturbation theory to isolate the most important coupling to the high-frequency modes, we found that the energy transfer to high-frequency modes is by Arnold diffusion, which depends exponentially on a frequency ratio as

$$\frac{dE}{dt} \propto \exp(-\pi \delta w_h / 2\Omega_B), \quad (2)$$

where  $\delta\omega_h$  is the difference frequency between two high-frequency modes. When  $\Omega_B \sim \delta\omega_h$ , the exponential factor is of order unity, allowing strong diffusion of energy to high-frequency modes, and equipartition on computationally observable time scales. Numerically, the transition to observable diffusion occurs at a value of  $E_c \approx 3$ , for  $\beta = 0.1$ , corresponding to  $\Omega_B / \delta\omega_h \approx 0.3$ . Since the coupling involves two high-frequency modes that initially have little energy, the resulting increase in energy is at first exponential, but later follows the usual diffusive scaling [8,9]. The scaling, with energy density, of the equipartition time for  $E \gg E_c$  has been found theoretically to be  $T_{eq} \propto (N/E)^3$ , which agrees with numerical computations.

The low-frequency modes of the FPU system, for  $\beta > 0$ , are approximately described by the modified Korteweg de Vries (mKdV) equation. An instability of a low-frequency soliton mode of the mKdV equation corresponds to the exponential growth in the FPU system [11]. The instability onset corresponds to  $R > 0.6$ , which is approximately the same value as that which produced a separatrix layer in the local resonance interaction. This is a necessary rather than sufficient condition for a transition to equipartition, as the soliton theory does not describe the high-frequency modes. However, it does present a physical picture of the process that holds the low-frequency modes together in the absence of perturbations (coupling to high-frequency modes). The processes that produce nonlinear structures become crucial when considering initial conditions in which energy is placed in high-frequency modes.

If the energy is initially placed in high-frequency modes, the equipartition process is significantly different from that starting from low-frequency initial conditions. In this case, the dynamics is transiently mediated by the formation of unstable nonlinear structures [12–16]. The mode energy is found to distribute itself first into a number of structures, localized in space, each consisting of a few oscillators, which coalesce over time into a single localized structure, a chaotic breather (CB). Over longer times, the CB is found to break up, with energy transferred to lower-frequency modes which do not have the breather symmetry. A transition with decreasing initial mode frequency is found such that the CB does not form, as expected from the loss of breather symmetry. For the FPU- $\beta$  chain, the scaling of CB formation time with energy density  $E/N$  is found numerically to be  $T_b \propto (E/N)^{-1}$ , and the scaling of equipartition time found to be  $T_{eq} \propto (E/N)^{-2}$  [14,16]. The scaling of  $T_{eq}$  can be predicted from the argument which postulates stochastic diffusion from high-frequency mode chaotic beat oscillations to the low-frequency modes, similar to that used for equipartition from low-frequency modes, given in [10]. The scaling of the time for the formation of a breather,  $T_b$ , can also be estimated from theory [15,16].

The mechanisms leading to equipartition are now reasonably understood for the FPU oscillator chain. However, a more complete understanding of the equipartition process requires a comparison to other coupled nonlinear oscillators. A particular system, well suited to such a comparison, is the discretized Klein-Gordon equation, consisting of nonlinear

oscillators linearly coupled to each other. For a quartic nonlinearity in the potential, the Hamiltonian is given by [17]

$$H = \sum_{i=1}^N \left[ \frac{1}{2} p_i^2 + \frac{1}{2} (q_{i+1} - q_i)^2 + \frac{m^2}{2} q_i^2 + \frac{1}{4} \beta q_i^4 \right], \quad (3)$$

which we henceforth call the  $\varphi^4$  system.

Recently, there have been a number of studies of the discretized Klein-Gordon equation, but they have been from the perspective of studying the stability of breathers, which are chosen as initial conditions [18,19]. However, it is clear from phase-space arguments that an initial condition that is a high-frequency linear mode, that subsequently forms breathers, cannot form stable breathers and therefore must ultimately decay. This was recognized in [13,14] for the FPU system and the processes of formation and decay were studied. An earlier study of the  $\varphi^4$  model compared numerical results of a transition from slow diffusion (long times to approach equipartition) to fast diffusion (short times to equipartition) with numerical results from the FPU model [17]. The only theory at that time was for the energy required for mode overlap [4], which does not consider the more subtle transitions and time scales, that occur at lower energy due to beat modes and breather decay, as described above.

In this paper, we investigate the  $\varphi^4$  system, comparing the numerical results to those of the FPU- $\beta$  chain, using the theory developed by us for the FPU studies, to understand the similarities and differences. In particular, we will be concerned with the transitions between exponentially slow time scales to approach equipartition and time scales governed by power laws. As with the FPU system, we calculate the energy density power-law scaling of the equipartition time and compare with numerical results. In this paper, we treat low-frequency initial conditions (LFIC). In a subsequent paper, we will consider high-frequency mode initial conditions. The comparisons with our theoretical and numerical work on the FPU system should distinguish between transitions and time scales that are universal and those that are model dependent.

## II. SOME THEORETICAL CONSIDERATIONS

A useful way of observing the dynamical motion numerically, mentioned in the Introduction, is to Fourier transform the oscillator coordinates to the normal modes of a chain containing only the linear restoring forces. This expansion describes the complete nonlinear system well, provided the energy in the linear terms is large compared to the energy in the nonlinear terms. As we shall see, the transformation works well over the interesting and numerically accessible energy ranges of the FPU chain, but has a much more limited range of validity for the  $\varphi^4$  chain. The harmonic part of the Hamiltonian can be put in the form of  $N$  independent normal modes  $Q_k$  via a canonical transformation, which for fixed end-point boundary conditions gives

$$q_i = \sqrt{\frac{2}{N+1}} \sum_{k=1}^N Q_k \sin\left(\frac{ik\pi}{N+1}\right), \quad (4)$$

which holds for both Hamiltonians (1) and (3). The above transformation puts the Hamiltonians in the form

$$H = \sum_{k=1}^N \frac{1}{2} (P_k^2 + w_k^2 Q_k^2) + \frac{\beta}{(8N+8)} \sum_{i,j,k,l=1}^N C(i,j,k,l) Q_i Q_j Q_k Q_l, \quad (5)$$

with the  $w_k$  given by

$$w_k = \sqrt{m^2 + 4 \sin^2 \left( \frac{\pi k}{2N+2} \right)}; \quad (6)$$

for the  $\varphi^4$  system, and

$$w_k = 2 \sin \left( \frac{\pi k}{2N+2} \right) \quad (7)$$

for the FPU system. The quartic coefficients for the  $\varphi^4$  system are given by

$$C(i,j,k,l) \equiv \sum_P B(i+j+k+l), \quad (8)$$

with  $P$  representing the eight permutations of sign of  $i,j,k,l$  and the function  $B(x)$  takes the value 1 if the argument is zero,  $-1$  if the argument is  $\pm 2(N+1)$ , and zero otherwise. In contrast, the coupling for the FPU has the form

$$C(i,j,k,l) \equiv w_i w_j w_k w_l \sum_P B(i+j+k+l), \quad (9)$$

i.e., the nonlinear terms get multiplied by the factor  $w_i w_j w_k w_l$ .

From the above, it is apparent that the FPU and the  $\varphi^4$  models differ in some significant ways. In the linear frequencies, there is an extra parameter  $m$  in the  $\varphi^4$  model, which flattens the low-frequency portion of the dispersion relation if  $m$  is of order one, while the FPU frequencies always start with nearly linear increments from the value  $w_1 = \pi/N + 1$ . In the quartic terms, from Eq. (9), we see that the terms in the FPU model are multiplied by an extra product of four frequencies, which is not present in the  $\varphi^4$  model. This causes the quartic  $\varphi^4$  terms to be much larger for the low-frequency modes than the corresponding low-frequency modes for the FPU system at the same energy density. To explore these differences in more detail, we transform to action-angle variables,  $I_i, \phi_i$ , for the harmonic part, using

$$Q_i = (2I_i/w_i)^{1/2} \cos(\phi_i), \quad P_i = (2w_i I_i)^{1/2} \sin(\phi_i), \quad (10)$$

to obtain the Hamiltonian

$$H = \sum_i w_i I_i + \left( \frac{\beta}{2N+2} \right) \sum_{i,j,k,l} \text{ang}(ijkl) \times \frac{C(i,j,k,l)}{\sqrt{w_i w_j w_k w_l}} (I_i I_j I_k I_l)^{1/2}, \quad (11)$$

where  $\text{ang}(ijkl) \equiv \cos(\phi_i) \cos(\phi_j) \cos(\phi_k) \cos(\phi_l)$ . The frequency of mode  $i$  is the derivative of the Hamiltonian with respect to  $I_i$ , giving

$$\Omega_i = w_i + \left( \frac{\beta}{2N+2} \right) \sum_{j,k,l} \text{ang}(ijkl) \times \frac{C(i,j,k,l)}{\sqrt{w_i w_j w_k w_l}} \left( \frac{I_j I_k I_l}{I_i} \right)^{1/2}. \quad (12)$$

Equations (11) and (12) differ for the  $\varphi^4$  chain, from the corresponding equations of the FPU chain, by the factor  $(w_i w_j w_k w_l)^{-1}$ . Thus, for small  $w$  the nonlinear frequency shift is much larger for  $\varphi^4$ . An estimate of the time average of the nonlinear frequency shift can be made as follows. Assuming that some  $\delta k$  modes contain energy, and noticing that the selection rule reduces the number of indices to be summed by one, we find that there are  $(\delta k)^2$  terms that can contribute to the above sum. After averaging over phases, the only nonzero terms are those which have a resonance among the four angles. The number of such resonances is linear in  $\delta k$ , such that only a group of terms proportional to  $\delta k$  actually contributes. Assuming that the terms are typically of the same size,  $w_i I_i \simeq E/\delta k$ , and the  $\delta k$  cancels. With these assumptions and taking the  $w_i$ 's to have approximately equal values,  $\delta k \ll N$ , then Eq. (12) yields

$$\delta w_{NL} \simeq \frac{\beta E}{N} \frac{1}{w_\gamma^3}, \quad (13)$$

for the time average of the nonlinear frequency shift, whose inverse defines an important time scale.

We now estimate the region of validity of the expansion by comparing the linear frequency  $w_i$  to the shift in frequency due to the nonlinearity  $\delta w_{iNL}$ . Since the nonlinear shift depends on the frequencies of the coupled modes, which are approximated by their linear parts, the expressions are valid for  $\delta w_{iNL}/w_i \ll 1$ . For an initial mode  $\gamma$ , Eq. (13) predicts

$$\frac{\delta w_{\gamma NL}}{w_\gamma} \sim \left( \frac{\beta E}{N} \right) \left( \frac{1}{w_\gamma} \right)^4, \quad (14)$$

with  $\gamma$  a typical mode in the  $\delta k$  packet of modes containing the energy. This same approximation for the FPU yields more simply

$$\frac{\delta w_{\gamma NL}}{w_\gamma} \sim \left( \frac{\beta E}{N} \right). \quad (15)$$

The implications of Eqs. (14) and (15) are quite different for the two models. For  $\delta w_{\gamma NL}/w_\gamma \ll 1$ , in the FPU-  $\beta$  system implies that  $\beta E/N \ll 1$ . This was assumed in all of our previous work [8–10]. For  $\varphi^4$ , on the other hand, the condition depends explicitly on the the linear frequency range under consideration. This difference was pointed out in [17], but the full implications were not explored. For  $m \ll 1$  and a low-frequency mode packet  $\pi \gamma/N \ll 1$ , the range of validity of the normal mode analysis of the  $\varphi^4$  chain is much more

restrictive. For example, with  $m=0.1$  and  $\pi\gamma/N\sim 0.1$ , a case treated numerically, we find  $\beta E/N < 4.0 \times 10^{-4}$  for our expansions to be valid. This region is hard to reach numerically and may effect the comparison of numerics with analytical estimates. This restriction is not severe for large values of  $m$ , or for high frequencies where  $w_\gamma \approx 2$  (with  $m$  small). Also, the calculations that we use to estimate  $T_{eq}$  may not depend critically on the validity of the expansion for the initial conditions, because the energy may spread over a larger number of nearby modes.

Continuing the argument for the  $\varphi^4$  model, as developed in [10] for the FPU model, we might expect that the beat frequency  $\Omega_B$ , which is driving the Arnold diffusion from the low frequency to other modes is related to the nonlinear frequency shift  $\Omega_B \sim \delta w_{\gamma NL}$ . This result was previously found to hold for the FPU chain, with a numeric factor significantly less than one [8].

### III. NUMERICAL RESULTS

We present numerical results for the  $\varphi^4$  oscillator chain, with selective comparisons to previous FPU results. The theory that is needed to understand these results, and comparison of theory with numerics will be presented in the following section.

All of our numerical integrations were performed with a recently developed tenth-order symplectic Runge-Kutta-Nystrom integrator [20], which is faster than previously used integrators. The high-order integrator can take very large steps, of about 0.6 of the shortest linear period and still conserves energy with a precision of  $10^{-10}$  even after integration times of  $10^{10}$ .

#### A. Macroscopic quantities

In numerical experiments, the instantaneous values of the linear energies  $E_i$ , of the linear modes, where the  $E_i$  are the quadratic terms in (5),  $i=1, \dots, N$ , is usually calculated. Over short times, the instantaneous and average values are nearly the same. The information entropy is defined by

$$S = - \sum_{i=1}^N e_i \ln e_i, \quad (16)$$

where  $e_i = E_i / \sum_i^N E_i$  are the normalized instantaneous energies. Two normalized measures of equipartition have been employed. The first employed measure is [5–7,17]

$$\eta \equiv \frac{S_{\max} - S(t)}{S_{\max} - S(0)}, \quad (17)$$

where  $S_{\max} = \ln(N)$  (equipartition). We see from the above definition that  $\eta = 1$  when  $S(t) = S(0)$  and  $\eta \rightarrow 0$  as  $S(t) \rightarrow S_{\max}$ , although fluctuations limit  $\eta$  to some finite value [15]. For  $N$  large and the initial energy in a few modes,  $\eta$  does not distinguish between equipartition and a plateau in which only some small number of the  $N$  modes are occupied, but is well behaved if some fixed fraction of the  $N$  initial

modes are excited. An alternative measure defines the effective number of modes sharing energy by [8–10,14,16]

$$N_{eff} = \exp(S), \quad (18)$$

which behaves well in the limits. The normalized parameter  $n_{eff} \equiv N_{eff}/N$  is related to  $\eta$ , for a single mode initial condition, through

$$\eta = \frac{\ln(N) - \ln(N_{eff})}{\ln(N)}. \quad (19)$$

We see that  $\eta \rightarrow 0$  as  $n_{eff} \rightarrow 1$ , but  $\eta$  also becomes small as  $N$  becomes large, even if  $n_{eff}$  is significantly less than one. The instantaneous value of  $n_{eff}$  does not asymptote to one, due to fluctuations. To calculate the effect of fluctuations we introduce a deviation  $\delta e_i$  from equipartition  $e_i = \bar{e} + \delta e_i$ . Substituting this into Eq. (18), expanding the logarithm function as  $\ln(1 + \delta e_i/\bar{e}) = \delta e_i/\bar{e} - (1/2)(\delta e_i/\bar{e})^2$  and performing the summation over  $i$  yields

$$\begin{aligned} n_{eff} &= \frac{1}{N} \exp\{-N\bar{e}\ln(\bar{e}) - N(\delta\bar{e})^2/(2\bar{e})\} \\ &= \exp\{-N(\delta\bar{e})^2/(2\bar{e})\}. \end{aligned} \quad (20)$$

Taking  $\bar{e} = 1/N$  and making the assumption of normal statistics, that for each normal mode  $(\delta\bar{e})^2 = \bar{e}^2$  (this is confirmed by calculations), we see that  $N$  cancels giving an asymptotic value  $n_{eff} = \exp(-0.5) = 0.61$ . This calculation shows that the result does not depend on the number of oscillators if  $N$  is large and also shows why the value is different from unity. The same calculation can also be made for oscillators, calculating the oscillator energies  $E_i$  directly from Eqs. (1) or (3) normalizing as for modes, and then using the normalized linear oscillator energies  $e_i$  in Eq. (16), one can calculate  $N_{osc}$  as in Eq. (18), with  $n_{osc} = N_{osc}/N$ . The resulting  $n_{osc} = 0.61$  at equipartition, from Eq. (20), which is the same as  $n_{eff}$ .

More accurate calculations have been made separately for modes and oscillators, including the nonlinear terms in the oscillator calculation, yielding [16]

$$n_{eff} = 0.65, \quad n_{osc} = 0.74 \quad (21)$$

at equipartition. These values have been checked numerically, giving good agreement [16]. Values of  $T_{eq}$  that have error bars are due to extrapolation or some other uncertainty. A comprehensive statistical analysis has not been performed due to the very long times for some runs. Spot checks for a few cases indicate that the spread from varying initial phases is not large. We use a logarithmic scale for the increasing time, in natural units of Eq. (3). The large fluctuations of the instantaneous values are smoothed by taking the average of the last five instantaneous values of  $n_{eff}$ , which are evaluated at a rate of 25 points per decade in time [at every integer value of  $25\ln(t)$ ].

We are now in a position to numerically determine the time scale to equipartition. However, before doing this it is



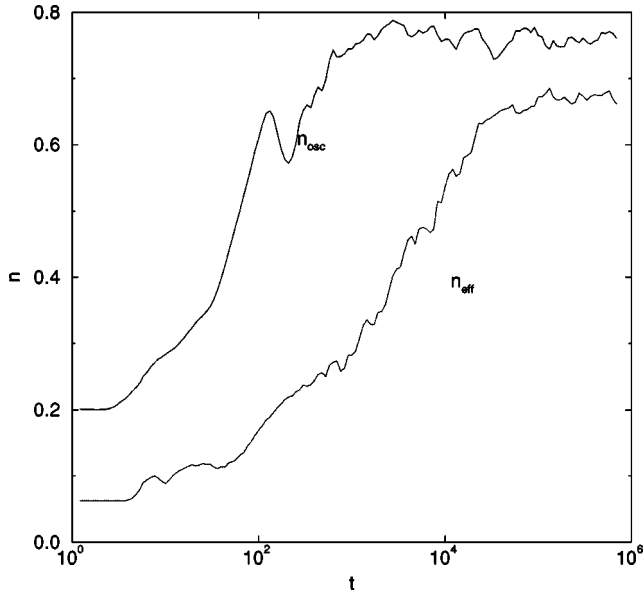


FIG. 1. For  $N=128$ ,  $m=0.1$ , and  $\varepsilon=E/N=0.05$ ,  $n_{eff}(t)$  and  $n_{osc}(t)$ , showing the saturation at  $t=T_{eq}$  with  $n_{eff}\approx 0.65$  and  $n_{osc}\approx 0.75$ . The time  $t$  is in natural units and the initial number of modes  $2\gamma=8$ , unless specified otherwise.

useful to find the most appropriate presentation of our data. We concentrate our attention on the  $\varphi^4$  chain, but will also compare  $\varphi^4$  results to FPU results. In Fig. 1, taking a convenient case with  $\beta=0.1$ ,  $N=128$ ,  $m=0.1$ , and  $\varepsilon=E/N=0.05$ , we placed equal energies with random phases in the lowest eight modes and plot the values of  $n_{eff}$  and  $n_{osc}$ . For varying  $N$  values, we can either choose a fixed fraction of modes as initial conditions, or a fixed number of modes, whichever we find to better eliminate initial transients. We have chosen  $N_{init}=8$ , unless otherwise specified. In Fig. 1, the initial value of  $n_{eff}=8/128$  is maintained for a short time, then rises continuously, and finally fluctuates about the equipartition value of  $n_{eff}\approx 0.65$ . Similarly  $n_{osc}$ , starting from a higher value since many oscillators have initial energy, also rises continuously to somewhat above the equipartition value of  $n_{osc}\approx 0.74$ , then settles back at essentially the same time as  $n_{eff}$  reaches 0.65. The time to equipartition (first crossing of  $n_{eff}=0.65$ ) is  $T_{eq}\approx 2\times 10^4$ . In a similar manner, with the same  $N$  and  $\gamma$ , we plot  $T_{eq}$  versus  $\varepsilon$  on a log-log plot in Fig. 2 (stars). We use this presentation because, from our experience with the FPU chain, we expect a power-law function  $T_{eq}\propto\varepsilon^{-q}$ , over some parameter range, which we indeed find. We note two distinct power laws, one at lower values of  $\varepsilon$  with  $q\sim 2.5$  and one at higher  $\varepsilon$  with  $q\sim 1.5$ .

The slope becomes steeper at the lowest values of  $\varepsilon$ , which corresponds to a transition to exponential behavior, as found for the FPU chain. We will see this exponential variation, using another presentation, in Fig. 3. But first, on the same figure, with a particular value of  $\varepsilon=0.05$  and  $N/16$  initial modes, we indicate  $T_{eq}$  for  $N=64$  (squares). These values lie close to those value for  $N=128$ , agreeing with our expectations, as found for the FPU chain, that, given a fixed coefficient for the nonlinear term,  $T_{eq}$  is a function of  $\varepsilon$ ,

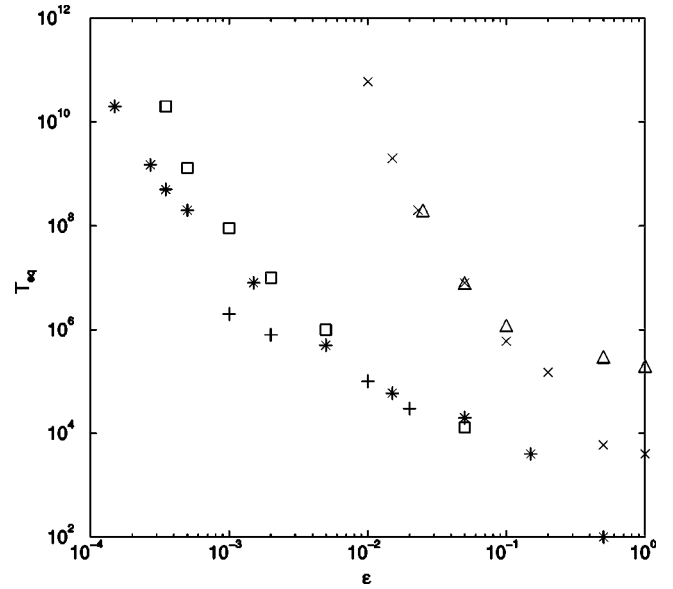


FIG. 2.  $T_{eq}$  vs  $\varepsilon=E/N$  on log-log scales with  $m=0.1, N=128$  (stars),  $N=64$  (squares), indicating power-law behavior independent of  $N$  except at small  $\varepsilon$ . Comparison with Ref. [17] (plusses), comparison with FPU,  $N=128$  (crosses),  $N=500$  (triangles).

only. However,  $n_{eff}(t)$  takes somewhat different paths to equipartition, indicating that there are  $N$ -dependent transients. From the values of  $T_{eq}$  for  $N=64$ , at the lower values of  $\varepsilon$ , we see that the  $N=64$  points break away from the  $N=128$  points to larger values of  $T_{eq}$  with decreasing  $\varepsilon$ . This behavior was found for the FPU, and for that system was understood in terms of a critical value of energy  $E_c$  for which the transition occurs. If the value of  $E_c$  is the same for any  $N$ , as it is in the FPU system, then the value of  $\varepsilon_c$  at which the transition takes place would vary inversely with  $N$  and therefore occur at a factor of 2 higher  $\varepsilon$  for  $N=64$  than for  $N=128$ . On the same figure, we plot values of  $T_{eq}$  for the FPU

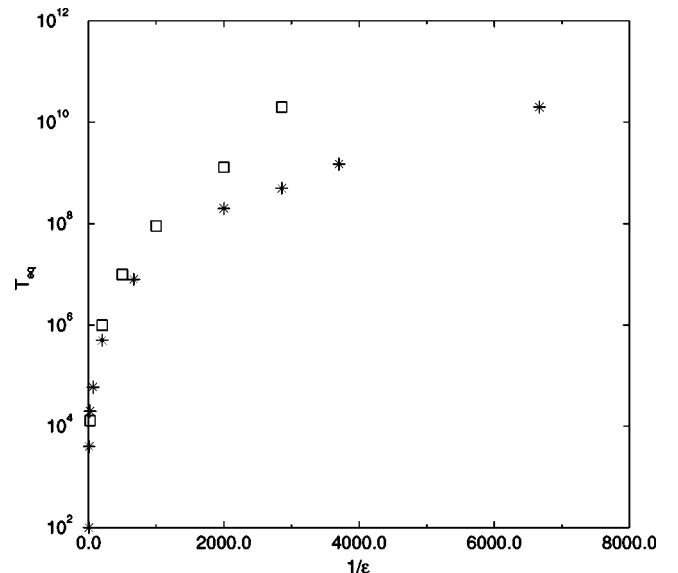


FIG. 3.  $T_{eq}$  on log scale vs  $1/\varepsilon$  to illustrate exponential behavior at small  $\varepsilon$ :  $N=128$  (stars),  $N=64$  (squares).

chain for  $N=128$  (crosses) and  $N=500$  (triangles). These results are similar to extrapolations from Fig. 5 in [10]. The slope has  $q \sim 3$ , as is also found theoretically in that paper. We see that a considerably larger  $\varepsilon$  is required to obtain the same  $T_{eq}$ . This can be understood qualitatively in terms of the larger nonlinearity at low frequencies for the  $\varphi^4$  system than for the FPU system. The results for the FPU with  $N=500$ , show that over the principal slope, the value of  $n_{eff}$  is intensive, i.e., not a function of  $N$  separately from  $\varepsilon = E/N$ . Similarly, we calculated a few values of  $T_{eq}(\varepsilon)$  for the  $\varphi^4$  with  $N=256, 500, 1000$ , and  $2000$ , (not shown) which lay close to the  $N=128$  values in the figure. Finally, we compared our results to values of  $T_{eq}$  reported in Fig. 7 of [17], at the same  $m$  value of  $0.1$ , but with slightly different  $N$  and initial conditions (plusses). The values lie significantly below our observed values, particularly at the smaller values of  $\varepsilon$ . We interpret this difference as at least partly due to the use of  $\eta$ , in [17], rather than  $n_{eff}$ , for determining  $T_{eq}$ , as we have discussed above.

In Fig. 3, we plot  $T_{eq}$  on a log scale versus  $1/\varepsilon$  (stars) for all  $\varepsilon$  values with  $N=128$ . If we are in the range in which the diffusion is exponentially slow (Arnold diffusion), then from the scaling in Eq. (2), with  $\delta w_h / \Omega_B \propto E^{-1}$  we expect to obtain a straight line for  $\log(T_{eq})$  versus  $1/\varepsilon$  if  $N$  is held constant. This is, indeed, found for four of the values, with a transition between  $\varepsilon = 10^{-3}$  and  $5 \times 10^{-4}$ . For  $N=128$  and  $5 \times 10^{-4} < \varepsilon < 10^{-3}$ , we have  $0.0614 < E < 0.128$ . This value is more than a factor of ten lower than the value of  $E_c \approx 3$  found for the FPU chain. In Fig. 3, we also plot (squares) the values of  $\varepsilon$  for  $N=64$ . As in Fig. 2, we see the transition from exponential  $T_{eq}$  versus  $1/\varepsilon$  to power-law behavior, with the transition occurring at a factor of 2 larger  $\varepsilon$  (a factor of 2 smaller value of  $1/\varepsilon$  in the figure).

We have also calculated  $T_{eq}$  with  $N=128$ , for  $m=0.025$  and  $m=0$ , for a few values of  $\varepsilon$  on the main slope. The values of  $T_{eq}$  fall on curves below that for  $m=0.1$ , and with different slopes, as might be expected from Eq. (6). For  $m=0.1$ , the linear frequency is affected by both the coupling term, and the linear self-forcing term. For cases in which we want the linear self-forcing term to be small, but sufficiently large to prevent large- $N$  problems, we have taken  $m=0.1$ , as was also used in [17].

If we take  $m=O(1)$ , the situation is considerably different. For this case, the linear frequency for low-frequency modes is dominated by the term including  $m$ , and the dispersion is quite different. This is seen from the frequencies in Eq. (6). The expansion procedure for the perturbed frequencies given by Eq. (12) is now valid to high energy. Although the nonlinear frequency shift is small compared to the linear frequencies, for low-frequency initial conditions, the differences between linear frequencies are small so that local overlap is easily achieved. This is easily seen by expanding and taking the difference for neighboring modes to obtain

$$\delta w_{\gamma L} \approx \frac{2}{m} \left( \frac{\pi}{2N} \right)^2 (2\gamma + 1) \quad (22)$$

and estimating the nonlinear frequency shift as in Eq. (14)

$$\frac{\delta w_{\gamma NL}}{\delta w_{\gamma L}} = \frac{2\beta E}{\pi^2 m^2} \frac{N}{(2\gamma + 1)}. \quad (23)$$

As in the FPU [8], from LFIC local overlap is obtained, at fixed  $\gamma$ , proportional to  $\beta EN$  and will generally occur at high  $N$ , even for small  $\beta E$ . This leads to a rapid spreading of the energy over some set of low-frequency modes. However, as also seen with the FPU, this does not imply equipartition on power-law times, as diffusion to high-frequency modes may be strongly impeded. In fact, the values of  $\varepsilon$  for which equipartition is observed are much higher for this case. A typical result is shown in Fig. 4, for  $\varepsilon=0.75$ , in which we plot  $n_{eff}(t)$  and  $n_{osc}(t)$ . We find a plateau in  $n_{eff}(t)$  is rapidly obtained. However, this macroscopic calculation does not tell us which modes contain the energy. The slower processes that can transport energy to high-frequency modes only manifest themselves on a much longer time scale. However, unlike high-frequency initial conditions, in which the intermediate time scale indicates the formation of transient localized structures [14–16], here, no such structures are formed, as seen from  $n_{osc}(t)$ , which does not drop to a low value on the intermediate time scale (the indication of breather formation).

In Fig. 5, we plot  $T_{eq}$  versus  $\varepsilon$  on log-log scales for  $m=1$  and  $N=128$  (pluses) and to confirm the  $\varepsilon$  scaling, also plot  $T_{eq}$  versus  $\varepsilon$  for  $m=1$  and  $N=256$  (stars). The close coincidence indicates that the  $\varepsilon$  scaling holds. There is also time spent on the plateau, before rising toward equipartition. We also checked the plateau times, again finding the coincidence. There is no induction period for sufficiently large  $\varepsilon$ . The disappearance of a transient state with increasing  $\varepsilon$  is also seen for high-frequency initial conditions in the FPU system [14,16].

Either because the dynamic range of  $\varepsilon$  is smaller and the points somewhat more varied, or because a transition has not been reached, there is no clear indication of a change from a power-law to exponential behavior. There is also a distinct change of the slope of  $\log(T_{eq})$  versus  $\log(\varepsilon)$  at about  $\varepsilon=1.5$ . This type of transition with increasing  $\varepsilon$  has been observed for small  $m$  [17] and for the FPU [5,6] and interpreted in those references as the onset of a strong overlap condition [4]. The lack of a clear transition between power-law and exponential behavior is made more apparent by plotting  $T_{eq}$  versus  $1/\varepsilon$ , on log-linear scale, in Fig. 6. We see that over the range of  $\varepsilon$  that was accessible, there is no clear separation between exponential and power-law behavior.

A recent numerical study of the scaling to equilibrium in the  $\varphi^4$  system was made over roughly similar values of  $0.03 \lesssim \beta E \lesssim 0.25$  but at much smaller values of  $\varepsilon$  since  $N$  was large (typically  $N=8192$ ) [21]. In that study, using various methods of estimating the time to equilibrium, but not measuring  $T_{eq}$  as done here, the conclusion was drawn that the equilibrium time increased exponentially as  $\exp[(\beta E)^{-\gamma}]$  with  $\gamma \approx 0.3$ . This would be consistent with our general expectations of exponential times, at these low values of  $\varepsilon$ , as we found for small  $m$ .

We also must check the scaling of  $T_{eq}$  with  $m$ . From our previous results using the FPU chain, we expect that a fun-

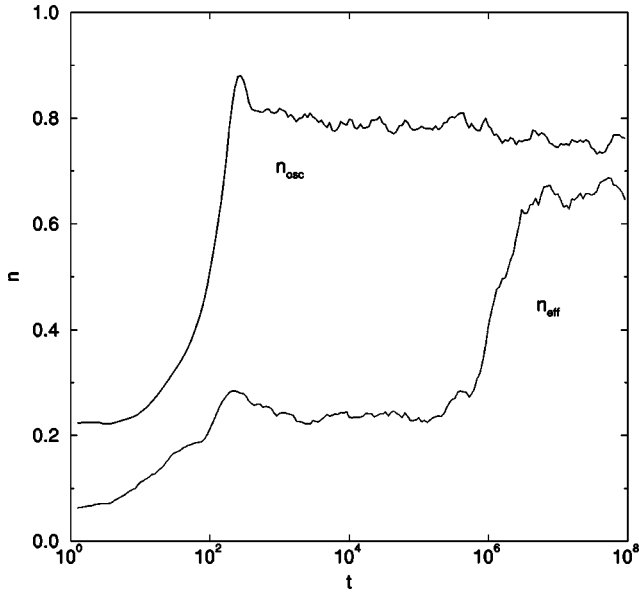


FIG. 4.  $n_{eff}(t)$  and  $n_{osc}(t)$  for  $N=128$ ,  $m=1$ ,  $\epsilon=0.75$  giving  $T_{eq}$  at  $n_{eff}\approx 0.65$ , but also showing an induction period on a plateau of  $n_{eff}$ . The time  $t$  is in natural units.

damental time scale is  $\Omega_B$ . From Eq. (13) assuming  $\Omega_B \propto \omega_{NL}$ , with  $m$  primarily determining the low-frequency mode frequencies, we might expect to obtain  $\epsilon/m^3$  scaling, but the theory does not give this value. In Fig. 7, we plot  $T_{eq}$  versus  $\epsilon/m^{2.75}$  for various values of  $m$ ; in particular for  $m=1$  (circles),  $m=0.75$  (stars),  $m=0.5$  (crosses), and  $m=0.25$  (triangles). We see that these values fit reasonably well on a single curve, with the power of  $m$  chosen to give the best fit. The scaling of the plateau height  $n_{eff}(p)$  with  $\epsilon$  and  $m$  can also be obtained from the same plots of  $n_{eff}$  versus  $t$  used to obtain Fig. 7. We present the data in Fig. 8,

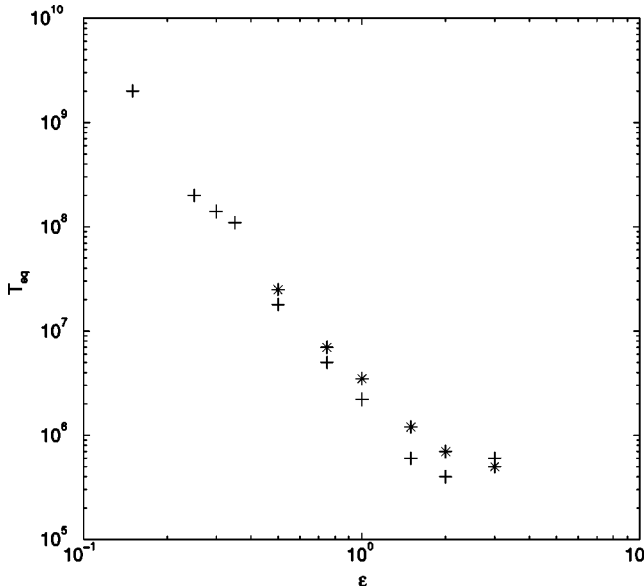


FIG. 5.  $T_{eq}$  vs  $\epsilon$  on log-log scales with  $m=1$ :  $N=128$  (pluses);  $N=256$  (stars); showing power-law behavior over a limited range of  $\epsilon$ .

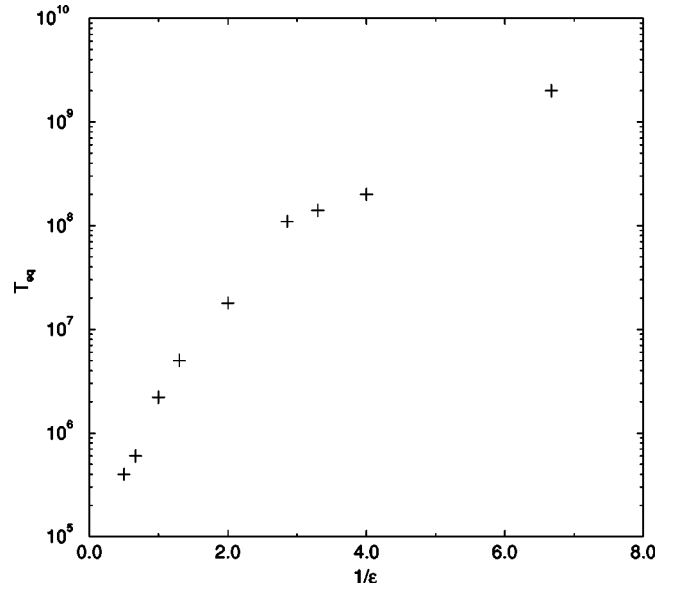


FIG. 6.  $T_{eq}$  on log scale vs  $1/\epsilon$ , for  $N=128$ ,  $m=1$ .

on a log-log scale of  $n_{eff}$  versus  $\epsilon/m^2$ , finding  $(\epsilon/m^2)^{1/2}$  scaling, where the power of  $m$  was chosen to bring the values of  $m$  close to a universal curve. There is a significant deviation of the  $\epsilon$  scaling at small  $n_{eff}$  which is getting closer to the initial value  $n_{eff}=0.062$ .

In all the above numerics, we have used eight initial low-frequency modes, with an implicit assumption that  $T_{eq}$  does not significantly depend on the number of initial modes, which mainly effects short-time transients. This is not entirely true, as we find a weak dependence of  $T_{eq}$  on the initial conditions. The height of the plateau, which is established early in time, depends more significantly on the initial conditions. We illustrate this in Fig. 9, with the results from two

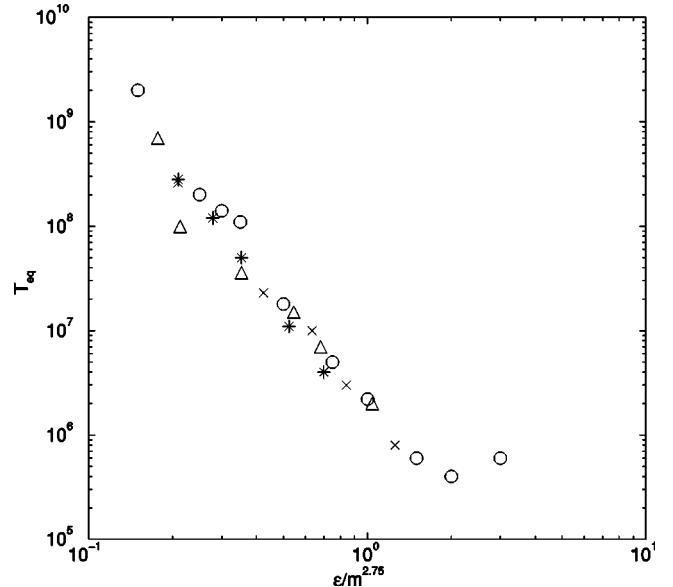


FIG. 7. Fitting  $T_{eq}$  to  $\epsilon/m^{2.75}$  on log-log scales for  $m=1$  (circles),  $m=0.75$  (stars),  $m=0.5$  (crosses), and  $m=0.25$  (triangles). Fitting to  $\epsilon/m^3$  gives almost as good a fit.

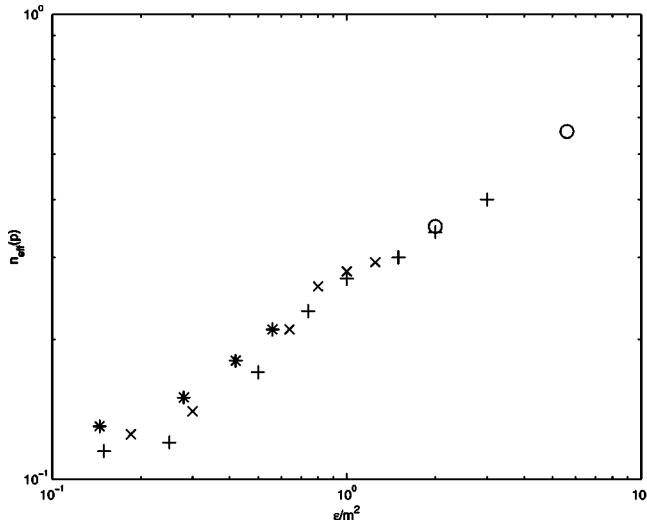


FIG. 8. Fitting  $n_{eff}$  (plateau) to  $\epsilon/m^2$  on log-log scales, for  $m=2$  (circles),  $m=1$  (plusses),  $m=0.75$  (stars), and  $m=0.5$  (crosses).

very different initial conditions,  $\gamma=3$  and  $\gamma=18$ , for a typical case of  $m=0.5$ , and  $\epsilon=0.06$ . We find  $n_{eff}(p)$  separated by a factor of about 3, while the values of  $T_{eq}$  are nearly the same. We also found for a few values at  $m>1$ , that there is increasing deviations from the  $m$  scaling as  $m$  is increased (but not the  $\epsilon$  scaling) from that given in Fig. 7.

The comparison of  $T_{eq}$  from  $\varphi^4$  with the the results from FPU show that for the same  $T_{eq}$  the  $\varphi^4$  values of  $\epsilon$  are generally more than a factor of 4 smaller than the FPU  $\epsilon$  values (Fig. 2). Although we are not studying high-frequency initial conditions (HFIC) in this paper, we have measured values of  $T_{eq}$  when the energy is initially placed in a few high-

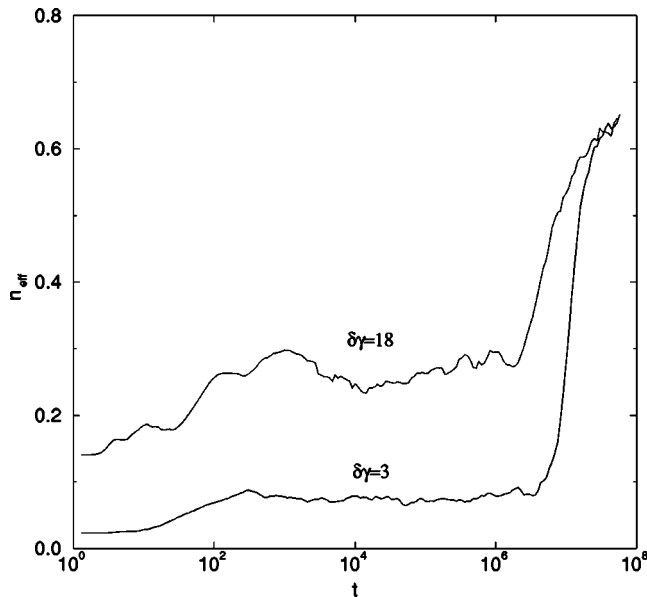


FIG. 9. Indicating the effect of initial conditions on  $T_{eq}$  and  $n_{eff}(p)$ , with  $m=0.5$  and  $\epsilon=0.062$ , for two initial conditions with  $\delta\gamma=3$  and  $\delta\gamma=18$ . For these cases, there is little effect of initial conditions on  $T_{eq}$ , but a rather strong effect on  $n_{eff}(p)$ .

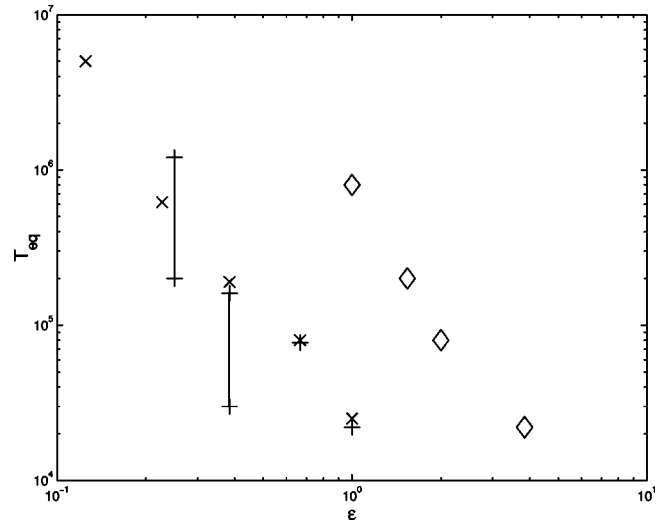


FIG. 10. Illustrating that for high-frequency initial conditions the value of  $T_{eq}$  vs  $\epsilon$  for the  $\varphi^4$  chain can be brought into coincidence with the FPU chain by choosing  $\beta=1.6$  rather than  $\beta=0.1$ , with the factor of 16 understood for from the strength of the nonlinear term at high-frequencies:  $\varphi^4$  (diamonds); FPU (crosses);  $\varphi^4$  with  $\beta=1.6$  (plusses).

frequency modes. In Fig. 10, these results are compared to the  $T_{eq}$  from the FPU model from [14]. We see the opposite characteristics from those in Fig. 2, with  $\epsilon$  larger by approximately a factor of 4 in the  $\varphi^4$  system (diamonds) than in the FPU system (crosses) for the same  $T_{eq}$ . This result can be explained by comparing the forms of the nonlinear terms in the two systems. For HFIC, the phases of neighboring oscillators alternate, and thus a quartic term is a factor of 16 larger for the FPU system, than for the  $\varphi^4$  system, which corresponds to a factor of 4 larger energy. This interpretation has been confirmed by increasing  $\beta$  by a factor of 16 for  $\varphi^4$ , bringing the  $T_{eq}$  values in close correspondence with those from the FPU system (plusses). From LFIC, the situation is reversed, with the nonlinear forces much smaller in the FPU system than in the  $\varphi^4$  system. [The large spread in the quoted  $T_{eq}$  for two points in Fig. 10 is due to an early peaking of  $n_{eff}(t) \approx 0.65$ , after which the value fell back and then climbed again to its final oscillation about  $n_{eff}(t) = 0.65$ . The upper times are probably more reliable, and lie close to the FPU values].

As we can see by comparing the  $T_{eq}$  in Fig. 5 for  $m=1$  with the values for  $m=0.1$ , in Fig. 2, the values of  $\epsilon$  required to obtain a given  $T_{eq}$  are orders of magnitude higher for  $m=1$  than for small  $m$ . Although there is strong overlap of modes at low frequency, for  $m=1$ , the ratio of the nonlinear frequency shift of a mode to the linear frequency of the mode is much smaller for  $m=1$  than for small  $m$ . The values of the linear frequencies for  $m=1$  are the same order of magnitude as the values of the linear high frequencies for any  $m$ , and we observe, by comparing the results of Fig. 5 with Fig. 10, that the values of  $\epsilon$  for LFIC at  $m=1$ , required to produce a given  $T_{eq}$  are quite similar to the values of  $\epsilon$  for HFIC for any  $m$ .



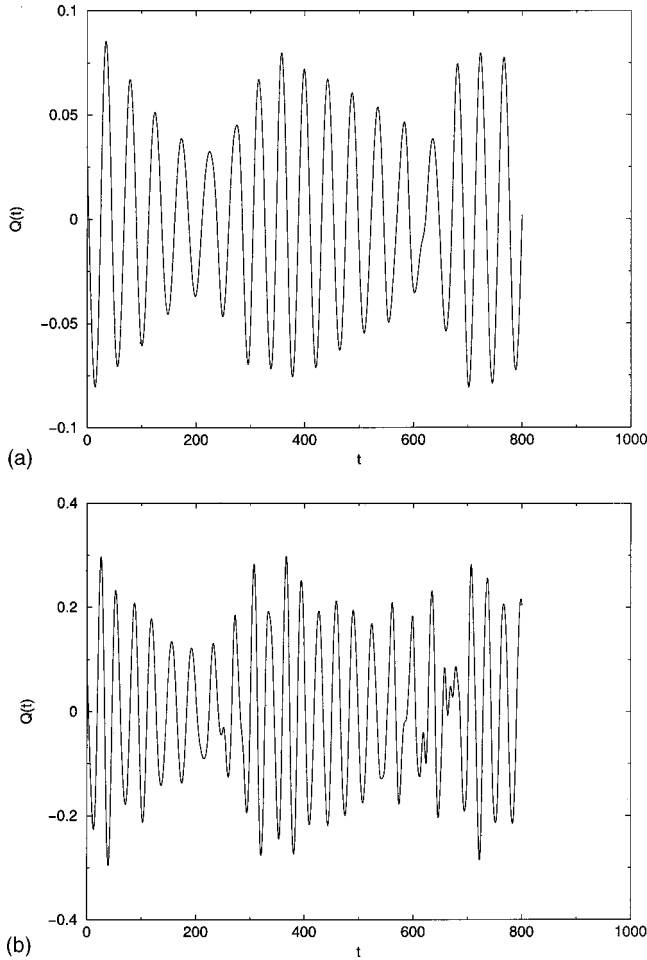


FIG. 11.  $Q(t)$  for mode 3, early in time with 90% of the energy initially in mode 3. (a)  $\epsilon = 0.0003$ , (b)  $\epsilon = 0.003$ . The change in frequency is seen and beats are also observed.  $Q$  is in arbitrary units.

### B. Microscopic quantities

To understand the underlying physics, we need to look more closely at the numerical evolution of more microscopic quantities. To investigate the validity of the approximations leading to the basic canonical forms we numerically calculate the primary frequencies of the modes. Examples of the oscillation of the amplitude of mode  $Q_i$  ( $i = \gamma$ ) is given in Fig. 11(a) for  $\epsilon = 3.0 \times 10^{-4}$  and in Fig. 11(b) for  $\epsilon = 3.0 \times 10^{-3}$ . In both cases, 90% of the initial energy was placed in mode  $\gamma = 3$ , as has been done in previous FPU studies. Because of the low energies there is little initial diffusion so the fast frequency  $w_{NL}$  is relatively constant over the short observation time periods. However, we should note that the initial conditions used here are significantly different from those used to obtain  $n_{eff}(t)$ . In Table I the mode frequency shifts are given as functions of  $\epsilon$ . These are compared with the theoretical estimates using Eq. (13). For  $\gamma = 3$ , we have from (6)  $w_L = 0.124$  and use  $\delta w_{NL} = w_{NL} - w_L$  to obtain  $\delta w_{NL}(\text{num})$ . Using Eq. (13) with  $w = w_L = 0.124$  in the denominator we obtain  $\delta w_{NL}(w_L)$ . The comparison for  $m = 0.1$  indicates that the perturbation theory used to obtain Eq. (12), and therefore Eq. (13), gives reasonable agreement be-

TABLE I. Nonlinear frequency shifts.

$m = 0.1$			
$\epsilon$	$\delta w_{DL}(\text{num})$	$\delta w_{NL}(w_L)$	$\delta w_{NL}(w_{NL})$
$3.0 \times 10^{-4}$	0.014	0.016	0.012
$1.0 \times 10^{-3}$	0.033	0.053	0.026
$3.0 \times 10^{-3}$	0.064	0.158	0.045
$1.0 \times 10^{-2}$	0.112	0.525	0.076
$m = 1$			
$\epsilon$	$\delta w_{NL}(\text{num})$	$\delta w_{NL}(w_L)$	$\delta w_{NL}(w_{NL})$
0.25	0.08	0.025	0.025
0.5	0.14	0.05	0.05
1.0	0.19	0.1	0.1

tween numerics and simple theory where it applies (estimated at  $\epsilon \lesssim 4.10^{-4}$ ), but gives too large values of  $\delta w_{NL}$  when the nonlinear change of the frequency is significant compared to the linear frequency. An estimate using a nonlinear frequency can be made by solving  $\delta w_{NL} = \beta E / N w_{NL}^3$ , and is given in the last column. For  $m = 0.1$ , it is better but lacks full theoretical justification. Beat oscillations are also observed, with additional harmonics, but are difficult to interpret. For the case of  $m = O(1)$ , the difficulty in the expansions do not exist for most values of  $\epsilon$ , and we would expect to obtain reasonably good agreement. However, as we see in the second half of the table, the theory considerably underestimates the observed nonlinear frequency shifts, and it is not understood.

Another important microscopic quantity is the mode spectrum. This gives information as to how energy is transferred among modes to produce the macroscopic  $n_{eff}$ . To illustrate this we compare the mode spectrum for the case shown in Fig. 1, with  $m = 0.1$  and  $\epsilon = 0.05$  at  $n_{eff} = 0.25$ , in Fig. 12(a) to spectra for the cases of Fig. 4 with  $m = 1$  and  $\epsilon = 0.75$ , in Figs. 12(b) and 12(c), for two times near the beginning and near the end of the plateau, respectively, with  $n_{eff} \approx 0.25$  at both times. Since the energy on average is spread among 32 modes ( $0.25 \times 128$ ), the mean energy mode is 16. In Fig. 12(a), we find the peak energy near this mode, with considerable spreading above it. In contrast, in Fig. 12(b), the modes with most energy lie below mode 16, with some energy in many of the high-frequency modes. This contrast becomes stronger in Fig. 12(c), which indicates a contraction of the modes carrying most energy to lower modes, with increased, but still relatively small energy in most of the higher-frequency modes. This behavior will be used to guide the development of a calculation procedure in the next section.

### IV. THEORETICAL ESTIMATES

The  $\varphi^4$  oscillator chain presents some difficulties in analysis that are not present for the FPU chain. For small  $m$ , e.g.,  $m = 0.1$ , the nonlinear frequency shifts, and therefore the expected beat frequencies, tend to be large compared to the linear mode frequencies and to the differences between them. Consequently, we expect to have a group of low-frequency modes that are strongly interacting. For  $m = O(1)$ , another

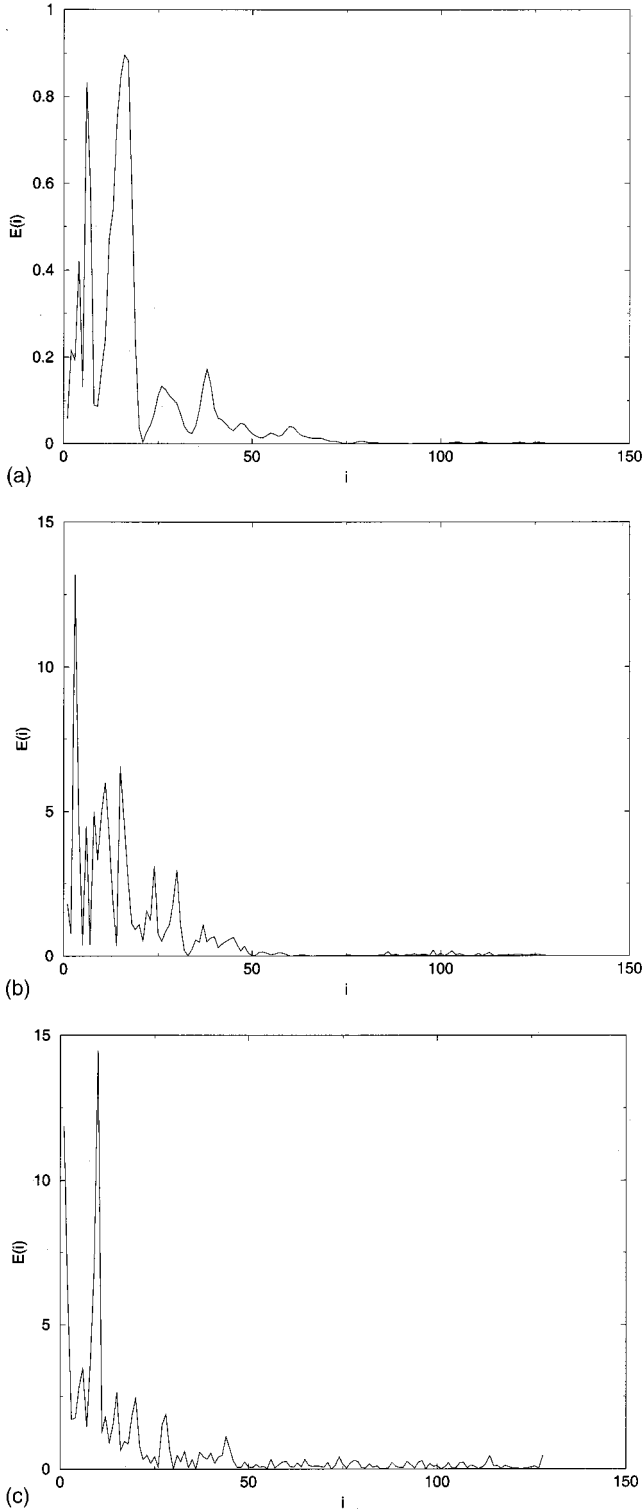


FIG. 12. Three-energy spectra at  $n_{eff} \approx 0.25$ ,  $N=128$ ,  $\delta\gamma=8$  (a)  $m=0.1$ ,  $\varepsilon=0.05$  (no plateau), (b)  $m=1$ ,  $\varepsilon=0.75$ , near the beginning of the plateau, (c) same as in (b) near the end of the plateau.  $E$  is in arbitrary units.

difficulty arises. The beat frequencies can be expected to be much smaller, but the low-frequencies are clustered about  $w=m$ , thus giving, again, a strong interaction among neighboring modes. Despite the problems in generalizing the

theory, first used in [10] for the FPU oscillator chain to estimate  $T_{eq}$ , we explore its use for the  $\varphi^4$  chain. Assuming the energy remains primarily in a group of modes, relatively small compared to the total number of modes, we differentiate Eq. (11) with respect to angle, to get the rate of change of the energy in that group. We use the assumption made in [10], that the phases are randomized in transferring energy from a driving mode to a set of driven modes, such that the summation in the nonlinear term gives a quantity proportional to  $\delta C$ , the square root of the number of couplings. Assuming energy transfer from a typical mode  $i$  to some effective package of modes, of frequency  $w_q$  with index  $k$ , where  $q=(\pi k/2N)$  is an intensive variable running from 0 to  $\pi/2$  used for clarity, then

$$\frac{dE_i}{dt} = -\frac{2\beta}{N} (\delta C) \frac{E_i}{w_\gamma} \frac{E_q}{w_q^2}, \quad (24)$$

where  $E_q$  is the energy of a typical mode in the driven group, assumed disjoint from the driving group. In Eq. (24), we take  $w_\gamma$  to be the frequency of the central mode of the driving package.

As we observed in describing the basic equations, the difference between the FPU quartic term and the  $\varphi^4$  quartic term is a factor consisting of a product of four frequencies. For a package of initially excited modes with approximately the same frequency and for  $m$  not too small, we assume the beat frequency to have the same scaling as the time average of the nonlinear frequency shift in Eq. (13)

$$\Omega_B \approx \left( \frac{\zeta}{w_\gamma^3} \right) \left( \frac{\beta E_p}{N} \right), \quad (25)$$

which is similar to the FPU results of [8] divided by the factor  $w_\gamma^4$ . Again,  $w_\gamma$  is taken to be the frequency of the central mode in the driving group (this approximate formula can not be used for  $m=0$  because some frequencies approach zero as  $N$  becomes large). The factor  $\zeta$  represents the reduction from the scaling in Eq. (13) due to phase averages and other factors, and we assume  $\zeta \approx 0.1$  in numerical calculations, consistent with such averaging. In Eq. (25),  $E_p$  is the total energy in the excited modes. Assuming that only the first  $2\gamma$  modes have a nonzero energy ( $E_p/2\gamma$ ), for  $m > \pi/N$  the dispersion relation of the  $\varphi^4$  system starts relatively flat at low-frequency, then has an intermediate region of more rapidly rising frequency per mode and becomes flatter at high-frequency.

We observe numerically, depending on the energy density, that there is often spreading from the low-frequency initial conditions to nearby low-frequency modes, on a time scale short compared to the equipartition time. It is this self-consistent package that drives the diffusion to the other modes. In the following, we determine the self-consistent size of the driving package by the hypothesis of a local overlap condition of the low-frequency modes that the energy will spread up to mode  $2\gamma$  for which the linear frequency spread ( $\delta w_L$ ) is equal to the beat frequency of Eq. (25). The hypotheses is tested by comparing the analytic results to the

numerics. Assuming sufficiently large  $m$  that all the low-frequencies in the driving package are given by  $w_\gamma \approx m$ , we expand the dispersion relation (6) to obtain  $\delta w_L = w_{2\gamma} - m$  as

$$\delta w_L = \frac{2\pi^2 \gamma^2}{mN^2}. \quad (26)$$

Making the strong assumption

$$\delta w_L = \Omega_B, \quad (27)$$

then, by equating Eqs. (26) to (25), we determine  $(\gamma/N)$  to be given by

$$\frac{\gamma}{N} = \left( \frac{\zeta \beta E_p}{2\pi^2 m^2 N} \right)^{1/2}. \quad (28)$$

If the value  $\gamma$  calculated by the above formula is less than the initial  $\gamma$ , then we can interpret Eq. (28) to mean that over short times the package size will be limited to its initial value. If Eq. (35) gives a  $2\gamma > \delta\gamma_{init}$  then the driving modes would be expected to grow to the size predicted by Eq. (28), again over a relatively short interval. With this interpretation in mind, assuming that the initial energy in the package is approximated as partitioned evenly among the modes

$$E_p = 2\gamma E_i, \quad (29)$$

we can calculate  $E_p$  by substituting Eq. (28) into Eq. (29)

$$E_p = \frac{2\zeta \beta N}{\pi^2 m^2} E_i^2, \quad (30)$$

and  $\gamma/N$  as a function of  $E_i$  by substitution of Eq. (30) into Eq. (28)

$$\frac{\gamma}{N} = \frac{\zeta \beta E_i}{\pi^2 m^2}. \quad (31)$$

Note that Eq. (31) implies that the number of driving modes shrinks during the equipartition process. Although the number of modes containing energy clearly increases, the two statements are not inconsistent as a minimum energy is required for driving other modes by the Arnold diffusion mechanism [8].

Because of the strong nonlinearity, the energy from the initial package typically goes from the driving modes to all other modes by Arnold diffusion. We use the following argument to determine the number  $\delta k$  of modes involved in the energy transfer: The linear beat  $\delta w_k$  is calculated using the dispersion relation  $w(q)$  of Eq. (6), where  $q = (\pi k/2N)$ , and taking  $dw/dq$  to be approximately constant over the interval,

$$\delta w_k \approx \left( \frac{dw_q}{dq} \right) \left( \frac{\pi \delta k}{2N} \right). \quad (32)$$

Here,  $\delta k$  and the effective center  $q$  of the resonant package are to be determined. We have used the linear beat in the approximation that the modes have very little energy for a

significant part of the transfer. As in the FPU calculation [10], we assume that the number of modes  $\delta k$  involved in the transfer can be determined as a function of the energy  $E_p$  in the driving package by the requirement of fast Arnold diffusion, which, from Eq. (2), is

$$\Omega_B(E_p) = \delta w_k. \quad (33)$$

Substituting Eqs. (25) and (32) into Eq. (33) determines  $\delta k$  to be

$$\delta k = \left( \frac{1}{dw_q/dq} \right) \left( \frac{2\zeta \beta E_p}{\pi w_\gamma^3} \right). \quad (34)$$

The number of couplings from a single low-frequency driving mode of index  $i$  to the outside resonant set of modes can be found by inspection of the selection rule: A mode  $\gamma_i$  of the driving package will couple to any pair of modes in the resonant package, of indices  $k_1$  and  $k_2$ , if we can find another driving mode, of index  $\gamma_j$ , such that the selection rule (8) is satisfied

$$\gamma_i - \gamma_j + k_1 - k_2 = 0. \quad (35)$$

It is important to notice here that we can satisfy the above selection rule for any  $k_1$  and  $k_2$  if the size  $2\gamma$  of the driving package is larger than the size  $\delta k$  of the driven package. In this case, there are  $(\delta k)^2$  couplings from each driving mode  $i$  to the driven package. For this condition to hold, Eqs. (27) and (33) together with the condition that  $2\gamma > \delta k$  imply that the driving modes must have  $dw/dk$  less than the driven modes, otherwise the theory must be modified.

Substituting  $\delta C = \delta k$  with  $\delta k$  given by Eq. (34) into Eq. (24) with  $E_p$  given by Eq. (30), and rearranging, we have

$$-m^4 \frac{dE_i}{E_i^3} = \left( \frac{8\zeta^2 \beta^3}{\pi^3 m^2 f_q} \right) E_q dt, \quad (36)$$

where we have substituted  $w_\gamma = m$  and  $f_q = w_q^2 dw_q/dq$ . As in [10] we make the simplest assumption of diffusive increase in the energy  $E_q$

$$E_q(t) = \frac{E}{N} \frac{t}{T_{eq}}. \quad (37)$$

Substituting Eq. (37) into Eq. (36), and integrating Eq. (36) with  $E_i$  going from  $E_i = (\pi^2 m^2 E/2\zeta \beta N)^{1/2}$  to  $E_i = (E/N)$  on the left side and  $t$  going from 0 to  $T_{eq}$ , averaging  $f_q$  over the whole spectrum

$$\langle f_q \rangle = \frac{2}{3\pi} (4+m^2)^{3/2}, \quad (38)$$

and dropping small terms, yields a formula for the dominant power law,

$$T_{eq} = \left( \frac{\pi^2 m^6}{12\zeta^2} \right) \frac{(4+m^2)^{3/2}}{\left( \frac{\beta E}{N} \right)^3}. \quad (39)$$

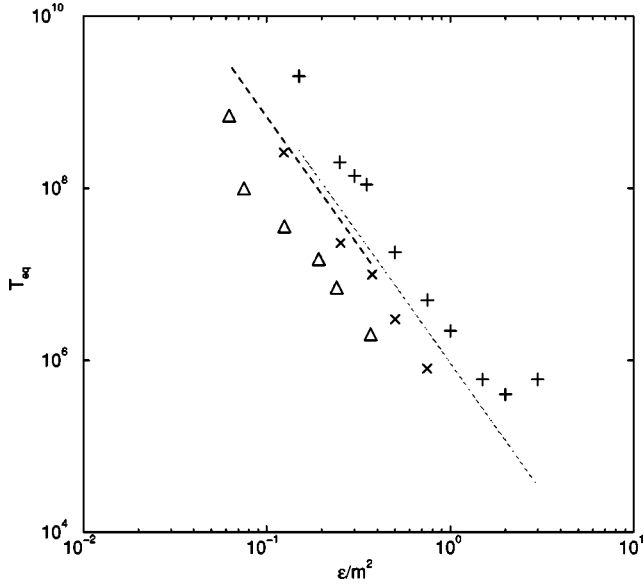


FIG. 13. Comparing the  $m$  and  $\varepsilon$  theoretical scaling with some  $m = O(1)$  numerics. The dominant theoretical value of  $\varepsilon/m^2$  is used in Eq. (39) for the theoretical calculation. The numerics are for  $m = 1$  (plusses),  $m = 0.5$  (crosses), and  $m = 0.25$  (triangles). The theory is for  $m = 1$  (solid line), and  $m = 0.25$  (dashed line).

Setting  $\zeta = 0.1$ , as discussed earlier, we compare Eq. (39) to the numerical results, for  $0.25 \leq m \leq 1$ , in Fig. 13, using the  $(\varepsilon/m^2)$  scaling of (39) ( $\varepsilon = E/N$ ). We note that the  $(\varepsilon/m^2)$  scaling of Eq. (39) is not a very good fit to the data, indicating the approximateness of our theoretical model in various respects. However, we stress that Eq. (39) makes sense in the thermodynamic limit of  $N \rightarrow \infty$ , as  $T_{eq}$  depends only on the energy density  $\varepsilon$ . We also note that  $T_{eq}$  is a function of  $\beta E$ , as it must be because of an exact symmetry of Hamiltonian (3) that allows a scaling of time to be compensated by a scaling of energy if  $\beta E$  is kept constant.

We can also justify the approximations leading to Eq. (28), by observing that over short times we expect  $n_{eff} \sim 2\gamma/N$ . Using this proportionality we have, from Eq. (28), the short-time relation

$$n_{eff} \sim \left( \frac{2\zeta\beta E}{\pi^2 m^2 N} \right)^{1/2} \quad (40)$$

agreeing well with the proportionality, found in Fig. 8, for the height of the plateau.

If the initial number of modes containing energy is larger than the number of modes predicted from Eq. (28), with  $\gamma = \frac{1}{2}\delta\gamma_{init}$  and  $E_p = E$ , then  $\delta\gamma$  is initially larger (and probably always larger) than the  $\gamma$  obtained from Eq. (28). This may be the reason for the change in the power law observed for the  $m = 0.1$  results in Fig. 2. Furthermore, unlike the higher  $m$  case, for which there is a tendency for  $\gamma$  to contract, as seen in Fig. 10(b), for small  $m$ , the opposite tendency can be seen from Fig. 10(a). This might mean that the contraction of the number of driving modes, implied by Eq.

(28), does not occur. There is not, however, clear evidence for how the number of driving modes changes during the evolution of  $n_{eff}$ .

## V. CONCLUSIONS AND DISCUSSION

We have examined the times to obtain energy equipartition in a discretized Klein-Gordon equation with strong quartic nonlinearity, called the  $\varphi^4$  oscillator chain. The results, both numerically and analytically, are compared to our previous results for the FPU oscillator chain, also with a strong quartic nonlinearity. The comparison, for this paper, is made primarily for energy initially placed in the low-frequency modes of the linearized systems. The  $\varphi^4$  oscillator chain is more complicated than the FPU chain, both because it has a separate parameter, the linear restoring force of the individual oscillators, and because the nonlinear forces tend to dominate the linear forces for the low-frequency modes. The extra parameter requires us to examine the behavior in a large parameter space.

For small linear restoring force,  $m = 0.1$ , of the individual oscillators [see Eq. (3) for the Hamiltonian] the linear frequencies of most modes are similar in the  $\varphi^4$  and FPU chains. The numerical calculation of  $T_{eq}(\varepsilon)$ , where  $\varepsilon = E/N$  the energy density of the chain, shows similar behavior of the two chains. Both have power-law behavior, depending only on  $\varepsilon$ , over a wide range of  $\varepsilon$ , and show  $N$ -dependent transitions at low  $\varepsilon$  to values of  $T_{eq}$  that increase much more strongly with decreasing  $\varepsilon$ , i.e.,  $T_{eq} \propto e^{a/\varepsilon}$ . The explanation for the transition, as related to Arnold diffusion, has been explored in detail in previous work on the FPU chain ([8]) and appears to hold for the  $\varphi^4$  chain, also. Nevertheless, even at relatively small  $m$ , there are important differences between the two chains, arising from the nonlinearity.

For larger  $m$ , the value of  $\varepsilon$  required to achieve a given  $T_{eq}$  is much larger. For a range of values  $0.25 \leq m \leq 1$ , the value of  $T_{eq}$  is found to scale as  $T_{eq} \propto (\varepsilon/m^p)^{-q}$  with  $p$  in the range from 2.5 to 3. The value  $p = 3$  could be argued as a scaling of the time with inverse beat frequency which has that scaling. A calculation of  $T_{eq}$  for  $m = O(1)$  predicted  $T_{eq} \propto (\varepsilon/m^2)^{-3}$ , where the power of  $q = 3$  agreed with the  $\varepsilon$  scaling found numerically while the power of  $p = 2$  was smaller than the numerical values.

Applying the theory to  $m = 0.1$  is less secure than that for  $m = O(1)$ , because the average frequency of the driving modes varies with  $\varepsilon$ , which induces a rather strong variation in the beat frequency. As the number of driving modes is uncertain, the average beat frequency is also uncertain, significantly affecting any calculation. The  $\varepsilon$  dependence of frequencies at small  $m$  would tend to decrease the power  $q$ , as observed for the  $m = 0.1$  case. However, the details are hard to establish firmly, from the theory.

We conclude that the general theoretical description of the various nonlinear dynamical mechanisms, describing the approach to equipartition in the FPU oscillator chain, hold approximately for the  $\varphi^4$  oscillator chain, provided  $m$  is not too small. The  $\varphi^4$  chain has a stronger nonlinearity, starting from



low-frequency mode initial conditions, which makes any analysis for small  $m$  less certain. For large  $m$ , there is both qualitative and quantitative comparisons between numerics and theoretical estimates to give some confidence in the underlying physics. The extra parameter in the  $\varphi^4$  chain has broadened the parameter space that we have studied, making a complete exploration of parameters more difficult. But within a limited range of the extra parameter, we have been able to get reasonable agreement between the numerics and

the theoretical estimates of  $T_{eq} \propto (\varepsilon/m^p)^{-q}$ , for the  $p$  and  $q$  powers.

#### ACKNOWLEDGMENTS

We thank Ch. Tsitouras for help in implementing the tenth-order integrator. We thank Steve Yoo for performing some of the numerical calculations. A grant from FAPESP supported a visit of J.DeL. to Berkeley, where the collaboration was begun.

- 
- [1] A. Lichtenberg and M. Lieberman, *Regular and Chaotic Dynamics*, 2nd ed. (Springer, New York, 1992), Sec. 6.5.
- [2] E. Fermi, J. Pasta, S. Ulam, and M. Tsingou, in *The Many Body Problem*, edited by D.C. Mattis (World Scientific, Singapore, 1993).
- [3] J. Ford, *J. Math. Phys.* **2**, 387 (1961); E. Atlee Jackson, *ibid.* **4**, 686 (1963).
- [4] F.M. Izrailev and B.V. Chirikov, *Dokl. Akad. Nauk (SSSR)* **57**, 166 (1966) [*Sov. Phys. Dokl.* **11**, 30 (1966)].
- [5] R. Livi, M. Pettini, S. Ruffo, M. Sparpaglione, and A. Vulpiani, *Phys. Rev. A* **28**, 3544 (1983); **31**, 1039 (1985); *J. Stat. Phys.* **48**, 539 (1987).
- [6] M. Pettini and M. Landolfi, *Phys. Rev. A* **41**, 768 (1990).
- [7] H. Kantz, R. Livi, and S. Ruffo, *J. Stat. Phys.* **76**, 627 (1994).
- [8] J. De Luca, A.J. Lichtenberg, and M.A. Lieberman, *Chaos* **5**, 283 (1995).
- [9] J. De Luca, A.J. Lichtenberg, and S. Ruffo, *Phys. Rev. E* **51**, 2877 (1995).
- [10] J. De Luca, A.J. Lichtenberg, and S. Ruffo, *Phys. Rev. E* **60**, 3781 (1999).
- [11] C.F. Driscoll and T.M. O'Neil, *Phys. Rev. Lett.* **37**, 69 (1976); *Rocky Mt. J. Math.* **8**, 211 (1978).
- [12] V.M. Burlakov, S.A. Kiselev, and V.I. Rupasov, *Phys. Lett. A* **147**, 130 (1990); V.M. Burlakov and S. Kiselev, *Zh. Eksp. Teor. Fiz.* **99**, 1526 (1991) [*Sov. Phys. JETP* **72**, 854 (1991)].
- [13] T. Cretegny, T. Dauxois, S. Ruffo, and A. Torcini, *Physica D* **121**, 109 (1998).
- [14] K. Ullman, A.J. Lichtenberg, and G. Corso, *Phys. Rev. E* **61**, 2471 (2000).
- [15] Yu.A. Kosevich and S. Lepri, *Phys. Rev. B* **61**, 299 (2000).
- [16] V.V. Mirnov, A.J. Lichtenberg, and H. Guclu, *Physica D* **157**, 251 (2001).
- [17] M. Pettini and M. Cerruti-Sola, *Phys. Rev. A* **44**, 975 (1991).
- [18] O. Bang and M. Peyrard, *Phys. Rev. E* **53**, 4143 (1996).
- [19] J.L. Marin and S. Aubry, *Nonlinearity* **9**, 1501 (1996); *Physica D* **119**, 163 (1998).
- [20] Ch. Tsitouras, *Celest. Mech.* **74**, 223 (1999).
- [21] G. Parisi, *Europhys. Lett.* **40**, 357 (1997).